Available online at www.eccomasproceedia.org
Eccomas Proceedia COMPDYN (2017) 4129-4144

ECCOMAS
Proceedia

COMPDYN 2017
6th ECCOMAS Thematic Conference on
Computational Methods in Structural Dynamics and Earthquake Engineering
M. Papadrakakis, M. Fragiadakis (eds.)
Rhodes Island, Greece, 15–17 June 2017

SEISMIC RELIABILITY-BASED DESIGN OF PERFECTLY ELASTOPLASTIC STRUCTURES ISOLATED BY FPS

P. Castaldo[1], B. Palazzo[2] and T. Ferrentino[3]

[1]Department of Structural, Geotechnical and Building Engineering (DISEG), Politecnico di Torino,
Corso Duca degli Abruzzi, 24, Turin, Italy (corresponding author);
e-mail: paolo.castaldo@polito.it; pcastaldo@unisa.it

[2]Department of Civil Engineering, University of Salerno,
Via Giovanni Paolo II (SA), Italy;
e-mail: palazzo@unisa.it

[3]Department of Civil Engineering, University of Salerno,
Via Giovanni Paolo II (SA), Italy;
e-mail tatianaferrentino@gmail.com

Keywords: seismic isolation; friction coefficient; seismic reliability; displacement ductility demand; strength reduction factor.

Abstract. *This paper deals with seismic reliability of nonlinear structural systems equipped with friction pendulum isolators (FPS). The isolated structures are described by employing an equivalent 2dof model characterized by a perfectly elastoplastic rule to account for the inelastic response of the superstructure, whereas, the FPS behavior is described by a velocity dependent model. An extensive parametric study is carried out encompassing a wide range of elastic and inelastic building properties, different seismic intensity levels and considering the friction coefficient as a random variable. Employing a set of natural seismic records and scaled to the seismic intensity corresponding to life safety limit state for L'Aquila site (Italy) according to NTC08, the inelastic characteristics of the superstructures are designed as the ratio between the average elastic responses and increasing strength reduction factors. Incremental dynamic analyses (IDA) are developed to evaluate the seismic fragility curves of both the inelastic superstructure and the isolation level assuming different values of the corresponding limit states. Integrating the fragility curves with the seismic hazard curves related to L'Aquila site (Italy), the reliability curves of the equivalent inelastic base-isolated structural systems, with a design life of 50 years, are derived proposing seismic reliability-based design (SRBD) abacuses useful to define the FPS properties and superstructure properties.*

Peer-review under responsibility of the organizing committee of COMPDYN 2017.
doi: 10.7712/120117.5711.16851

1 INTRODUCTION

In the last decades, friction pendulum system (FPS) has emerged as a very effective technique for the seismic isolation [1] of building frames due to its advantages, mainly related to the capability of providing an isolation period independent of the mass of the supported structure, its high dissipation and recentering capacity [2]-[3]. Over the years, within the issue of the passive control of structures, many works have developed new design strategies and methodologies [4]-[19] as well as probabilistic analyses in structural dynamics, structural reliability methods, and reliability-based analysis have been presented [20]-[30]. The influence of the friction pendulum system (FPS) isolator properties on the seismic performance of base-isolated building frames by employing 3D systems as well as two-degree-of-freedom (2dof) model accounting for the superstructure flexibility with a velocity-dependent model for the FPS isolator behaviour has been analyzed by Castaldo et al. [31]-[34]. In particular, seismic reliability analyses of a 3D r.c. elastic system isolated by FPS bearings have been carried out in [31]-[32] by accounting for the randomness of both the isolator properties (i.e., coefficient of friction) and of the earthquake main characteristics. The seismic reliability-based design approach has been proposed in [33]-[34] for elastic and inelastic systems isolated by friction pendulum devices.

With reference to the inelastic behavior of base-isolated systems under strong seismic events, seismic codes [35]-[38] provide design response spectra, defined by the ratio of elastic response spectrum ordinates to a parameter, called strength reduction factor [35],[39] or behaviour factor [36]-[37], usually defined, within a force-based design approach of new structures, as the product between two terms: ductility-dependent component and overstrength factor [39]. In particular, the Italian seismic code, NTC08 [37], the European seismic code Eurocode 8 [36] and the Japanese building code [38] provide a maximum behavior factor value of 1.5 for base-isolated structures, without explicitly distinguishing the different terms (i.e., ductility and overstrength factors). The US seismic design codes, ASCE 7 [35], prescribes the strength reduction factor for a seismically isolated structure to be 0.375 times the one for a corresponding fixed-base structure and no larger than 2.

The aim of this work is to propose reliability-based formulae for the preliminary design of base-isolated regular frames, located in an area characterized by a seismic hazard similar to the local seismic hazard of L'Aquila site (Italy). The results of the reliability analyses demonstrate that within the investigated parameter combinations the values of the strength reduction factor for base-isolated systems with FPS should be lower than 1.5.

2 INELASTIC MODEL OF A BASE-ISOLATED STRUCTURE WITH FPS

In this study the 2dof (degree-of-freedom) model proposed by Kelly [40], modified to account for inelastic responses of both the isolation level and the superstructure (Fig. 1), is adopted. The bearing response is modelled using a bilinear hysteretic response envelope, while the superstructure behaviour is described using a perfectly elastoplastic model. With reference to the symbols in Fig. 1, the equations of motion are:

$$\begin{aligned} &\left(m_b + m_s\right)\ddot{u}_b + m_s\ddot{u}_s + c_b\dot{u}_b + \frac{W}{R}u_b + \mu_d W \operatorname{sgn}\dot{u}_b = -\left(m_b + m_s\right)\ddot{u}_g \\ &m_s\ddot{u}_b + m_s\ddot{u}_s + c_s\dot{u}_s + f_s\left(u_s, \operatorname{sgn}\dot{u}_s\right) = -m_s\ddot{u}_g \end{aligned} \tag{1}$$

where $W=(m_b+m_s)g$ is the weight on the bearing, R is the radius of curvature of the FPS, μ_d is the bearing friction coefficient, that varies with the velocity according to Mokha et el. and Constantinou et el. [4]-[6]:

$$\mu_d = f_{\max} - (f_{\max} - f_{\min})\exp(-\alpha \dot{u}_b) \tag{2}$$

where f_{max} and f_{min} are the friction coefficient attained at high and at very low velocities of sliding respectively, α is a constant for a given pressure, temperature and condition of FPS interfaces. In this study, this constant equal to 30 and the ratio f_{max}/f_{min} equal to 3, based on regression of the experimental results [4]-[6], are assumed.

The superstructure is in the elastic phases if (3) is satisfied and the corresponding restoring force is given by (4).

$$\left|u_{s,i} - u_{0,i-1}\right| < u_y \text{ or } (f_{s,i-1} = f_y \,\&\, \dot{u}_{s,i}\dot{u}_{s,i-1} < 0) \tag{3}$$

$$f_{s,i}(u_s, \operatorname{sgn}\dot{u}_s) = k_s(u_{s,i} - u_{0,i-1}) \tag{4}$$

Otherwise, the superstructure is in the plastic phases if

$$\left|u_{s,i} - u_{0,i-1}\right| \geq u_y \tag{5}$$

$$f_{s,i}(u_s, \operatorname{sgn}\dot{u}_s) = f_y \operatorname{sgn}(u_{s,i} - u_{0,i-1}) \tag{6}$$

where i and $(i-1)$ indicate the time instants. The seismic isolation degree [41] is an indicator of the isolation system efficiency for elastic structures and results to be the ratio between the isolation $T_b=2\pi\sqrt{(m_b+m_s)/k_b}$ and superstructure $T_s=2\pi\sqrt{m_s/k_s}$ period of vibration: $I_d=T_b/T_s$. Regarding the inelastic response of a yielding superstructure (Fig. 1), characterized by a single degree of freedom with a perfectly elastoplastic behavior and assumed as the equivalent model representative of multi-story building frames [42]-[44], the corresponding strength reduction factor is defined as $q=f_{s,el}/f_y=u_{s,el}/u_y$, where $f_{s,el}$ and $u_{s,el}$ are, respectively, the minimum yield strength and yield deformation required for the superstructure to remain elastic during a ground motion, or the peak response values for the corresponding linear system. Note that q is different from the one provided by [35]-[39] because it does not explicitly consider the overstrength factor since the overstrength capacities are taken into account in the perfectly elastoplastic system assumed as equivalent model of the inelastic behavior of real multi-story building frames [39]; so q is related only to the ductility-dependent component [42]-[44].The displacement ductility, μ, of the superstructure is the ratio between the peak displacement of the inelastic system, $u_{s,max}$, and the yield displacement u_y. According to [40], the mass ratio $\gamma=m_s/(m_b+m_s)$, isolation $\xi_b=c_bT_b/[2(m_b+m_s)]$ and superstructure $\xi_s=c_sT_s/(2m_s)$ damping ratio are defined.

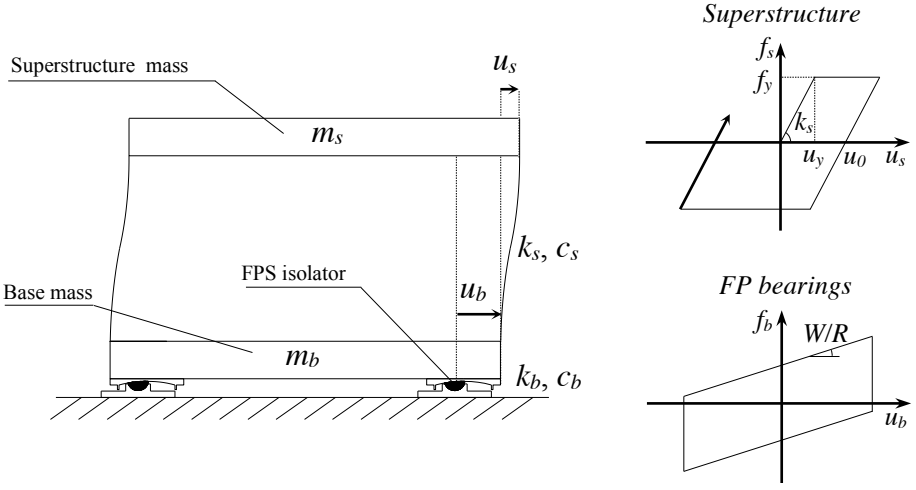

Figure 1: 2dof model of a building isolated with FPS.

3 UNCERTAINTIES CONSIDERED

Seismic reliability assessment of a building structure, according to the structural performance (SP) evaluation method [45]-[47], is based on the coupling between structural performance levels [48] and associated exceeding probabilities during its design life [49]-[50]. According to [51]-[53], the uncertainties related to the seismic input intensity are separated from those related to the characteristics of the record (record-to-record variability) by introducing a scale factor, called intensity measure (*IM*).

#	Year	Earthquake Name	Recording Station Name	Vs_{30} [m/s]	Fault Type	M [-]	R_s[km]	PGA [g]
1	1994	Northridge	Beverly Hills - Mulhol	356	Thrust	6.7	13.3	0.52
2	1994	Northridge	Canyon Country-WLC	309	Thrust	6.7	26.5	0.48
3	1994	Northridge	LA-Hollywood Stor	316	Thrust	6.7	22.9	0.36
4	1999	Duzce, Turkey	Bolu	326	Strike-slip	7.1	41.3	0.82
5	1999	Hector Mine	Hector	685	Strike-slip	7.1	26.5	0.34
6	1979	Imperial Valley	Delta	275	Strike-slip	6.5	33.7	0.35
7	1979	Imperial Valley	El Centro Array #11	196	Strike-slip	6.5	29.4	0.38
8	1995	Kobe, Japan	Nishi-Akashi	609	Strike-slip	6.9	8.7	0.51
9	1995	Kobe, Japan	Shin-Osaka	256	Strike-slip	6.9	46.0	0.24
10	1999	Kocaeli, Turkey	Duzce	276	Strike-slip	7.5	98.2	0.36
11	1999	Kocaeli, Turkey	Arcelik	523	Strike-slip	7.5	53.7	0.22
12	1992	Landers	Yermo Fire Station	354	Strike-slip	7.3	86.0	0.24
13	1992	Landers	Coolwater	271	Strike-slip	7.3	82.1	0.42
14	1989	Loma Prieta	Capitola	289	Strike-slip	6.9	9.8	0.53
15	1989	Loma Prieta	Gilroy Array #3	350	Strike-slip	6.9	31.4	0.56
16	1990	Manjil, Iran	Abbar	724	Strike-slip	7.4	40.4	0.51
17	1987	Superstition Hills	El Centro Imp. Co.	192	Strike-slip	6.5	35.8	0.36
18	1987	Superstition Hills	Poe Road (temp)	208	Strike-slip	6.5	11.2	0.45
19	1987	Superstition Hills	Westmorland Fire Stat.	194	Strike Slip	6.5	15.1	0.21
20	1992	Cape Mendocino	Rio Dell Overpass	312	Thrust	7.0	22.7	0.55
21	1999	Chi-Chi, Taiwan	CHY101	259	Thrust	7.6	32	0.44
22	1999	Chi-Chi, Taiwan	TCU045	705	Thrust	7.6	77.5	0.51
23	1971	San Fernando	LA - Hollywood Stor	316	Thrust	6.6	39.5	0.21
24	1976	Friuli, Italy	Tolmezzo	425	Thrust	6.5	20.2	0.35
25	1980	Irpinia	Bisaccia	496		6.9	21.3	0.94
26	1979	Montenegro	ST64	1083	Thrust	6.9	21.0	0.18
27	1997	Umbria Marche	ST238	n/a	Normal	6.0	21.5	0.19
28	2000	South Iceland	ST2487	n/a	Strike Slip	6.5	13	0.16
29	2000	South Iceland (a.s.)	ST2557	n/a	Strike Slip	6.4	15.0	0.13
30	2003	Bingol	ST539	806	Strike Slip	6.3	14.0	0.30

Table 1: Selected ground motions for the time history analyses.

The approach is based on calculating the probabilities of exceeding different limit state thresholds, properly defined, given different values of the intensity measure with the aim to define the fragility curves of the system. Afterward, the abovementioned fragility curves integrated with a seismic hazard curve, expressed in terms of the same *IM*, related to a reference site, lead to the mean annual rates of exceeding the limit states. Using a Poisson distribution, it is possible to transform the mean annual rates of exceeding the limit states into probabilities of exceedance in the time frame of interest (e.g., 50 years).

The aim of this work consists of evaluating the seismic reliability of inelastic structural systems equipped with friction pendulum isolators (FPS) considering both the friction coefficient and earthquake characteristics as random variables within the uncertainties relevant to the problem.

The spectral displacement, $S_D(\xi_b, T_b)$, at the isolated period of the system, T_b, and for the damping ratio, ξ_b, is assumed as intensity measure, *IM*. In the analyses carried out in this study, the damping ratio ξ_b is taken equal to zero, consistently with other works which assume that friction is the only source of damping in the isolators [54]. The corresponding *IM* is hereinafter denoted to as $S_D(T_b)$ and it is assumed ranging from 0.1 m to 0.45 m. The record-to-record variability is described through a set of 30 ground motion records, selected within the ground motion databases of PEER (Pacific Earthquake Engineering Research Center) [55], of ITACA (Italian Accelerometric Archive) [56] and of ISESD (Internet-Site for European Strong-Motion Data) [57]. The characteristics of the selected ground motion records are reported in Tab. 1. Their source-to-site distance, R_s, is greater than 8.7 km, and their moment magnitude, M, is in the range between 6 and 7.6.

As discussed in [4]-[6], the friction is a complex phenomenon and several mechanisms contribute to its variability. It follows that a Gaussian probability density function (PDF), interrupted from 0.5% to 5.5% with a mean value equal to 3%, is employed to model the friction coefficient at large velocity as random variable f_{max}. For the generation of 15 sampled values of f_{max} the stratified sampling technique the Latin Hypercube Sampling (LHS) method [31],[58]-[60] is adopted.

4 RELIABILITY ANALYSIS OF INELASTIC BASE-ISOLATED STRUCTURES WITH FPS

4.1 Parametric study

The first step to determinate the seismic reliability of the inelastic base-isolated equivalent systems consists of developing incremental dynamic analyses (IDAs) [61]. For this reason, an extensive parametric study is carried out encompassing a wide range of the parameter combinations related to isolation level and superstructure, according to Eqn. (1).

The deterministic parameters are: the isolation degree I_d, assumed equal to 6, the isolation period of vibration, T_b, varying between 3 s and 6 s, the mass ratio γ assumed equal to 0.6 and 0.8 and the (ductility-dependent) strength reduction factor q ranging from 1.1 to 2, corresponding to the values provided by the codes [35]-[38] for the behavior factor, in the case of unitary overstrength factor. Furthermore, the analyzed inelastic 2DOF systems have the isolation ξ_b and superstructure ξ_s damping ratio respectively equal to 0% and 2% and the seismic isolation degree I_d equal to 6.

In order to define the inelastic characteristics of each equivalent structural system, dynamic analysis of the base-isolated systems (defined for different values of T_b, γ and q), with a friction coefficient equal to 3%, have been subjected to the set of 30 seismic records, scaled to the *IM* value related to the life safety limit state (NTC08 [37]) for L'Aquila site (Italy): the *IM* is equal to 0.311 m for T_b=3, 4, 5 s (Fig. 2b) and equal to 0.26 m for T_b=6 s. The superstructure dynamic responses, expressed in terms of displacements relative to the base $u_{s,el}$, have allowed to evaluate the average yield displacement for each value of q. In this way, the inelastic characteristics of the equivalent structural systems have been defined.

4.2 Incremental dynamic analysis (IDA)

The above-mentioned equivalent structural systems, with the different structural parameters (T_b, γ, q) and combined for each value of the sampled friction coefficient, are subjected to the 30 ground motions, scaled to eight intensity levels values within the incremental dynamic analysis. The response parameters μ and $u_{b,max}=|u_b(t)|_{max}$, are adopted as the engineering demand parameters (EDPs) and assumed to follow a lognormal distribution. A lognormal distribution can be fitted to the both response parameters by estimating the sample lognormal mean, $\mu_{ln}(EDP)$, and the sample lognormal standard deviation $\sigma_{ln}(EDP)$, through the maximum likelihood estimation method.

The IDA results of the isolation level and the superstructure are plotted in Fig.s 2-3, in the form of meshes versus the intensity measure *IM* and the (ductility-dependent) strength reduction factor q. Each figure contains several surface plots, corresponding to the different values of the percentile and to both values of the mass ratio.

Fig. 2 shows the IDA results regarding the isolation level. The statistics of the EDP $u_{b,max}$ are influenced by T_b: the lognormal mean slightly decreases by increasing T_b, while the dispersion increases for higher T_b. Both the statistical values are also influenced by γ: the isolation displacement decreases by increasing γ. In fact, the mass ratio controls the contribution of the second mode of vibration to the response. This mode induces significant deformations in the superstructure only. On the other hand, the increase of q leads to a slight decrease of the displacement $u_{b,max}$.

Fig. 3 show the IDA curves regarding the superstructure. The increase of strength reduction factor q leads to a very high increase of the displacement ductility demand μ. The response parameter μ increases for increasing γ and for decreasing T_b.

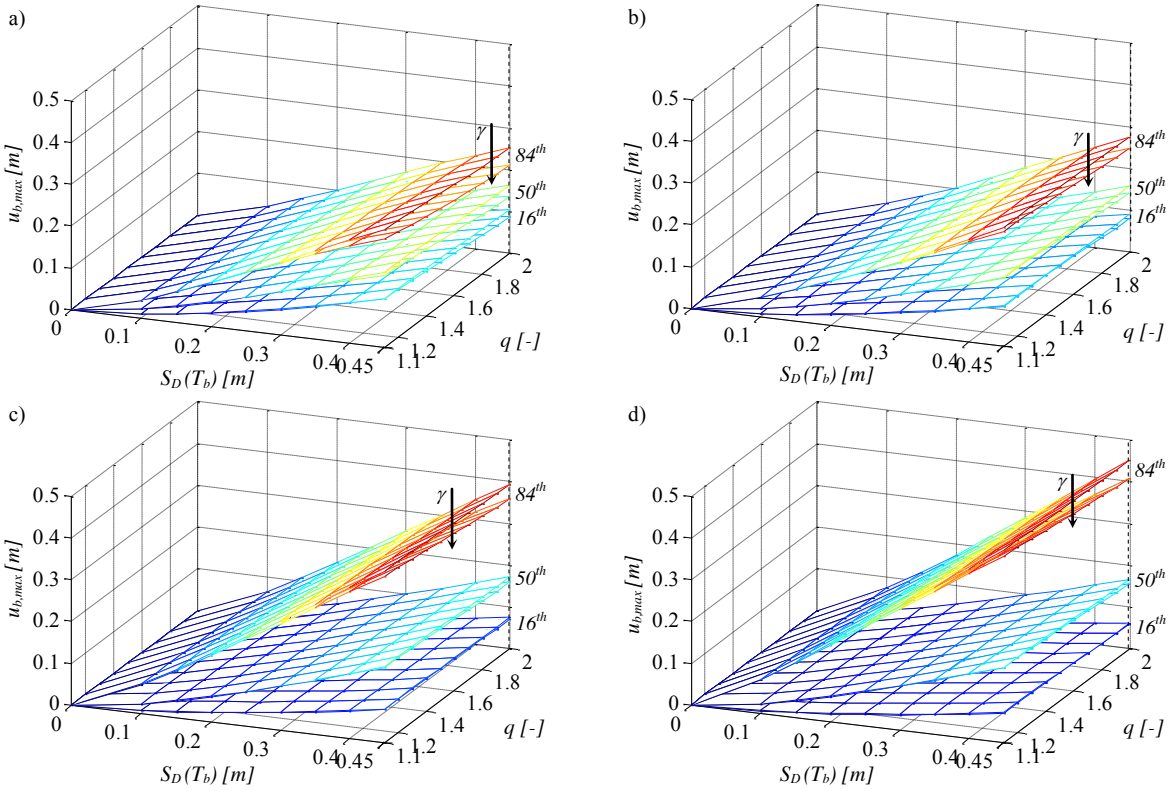

Figure 2: IDA curves of the isolation level with I_d=6 and T_b=3 s (a), T_b=4 s (b), T_b=5 s (c), T_b=6 s (d). The arrow denotes the increasing direction of γ = 0.6-0.8.

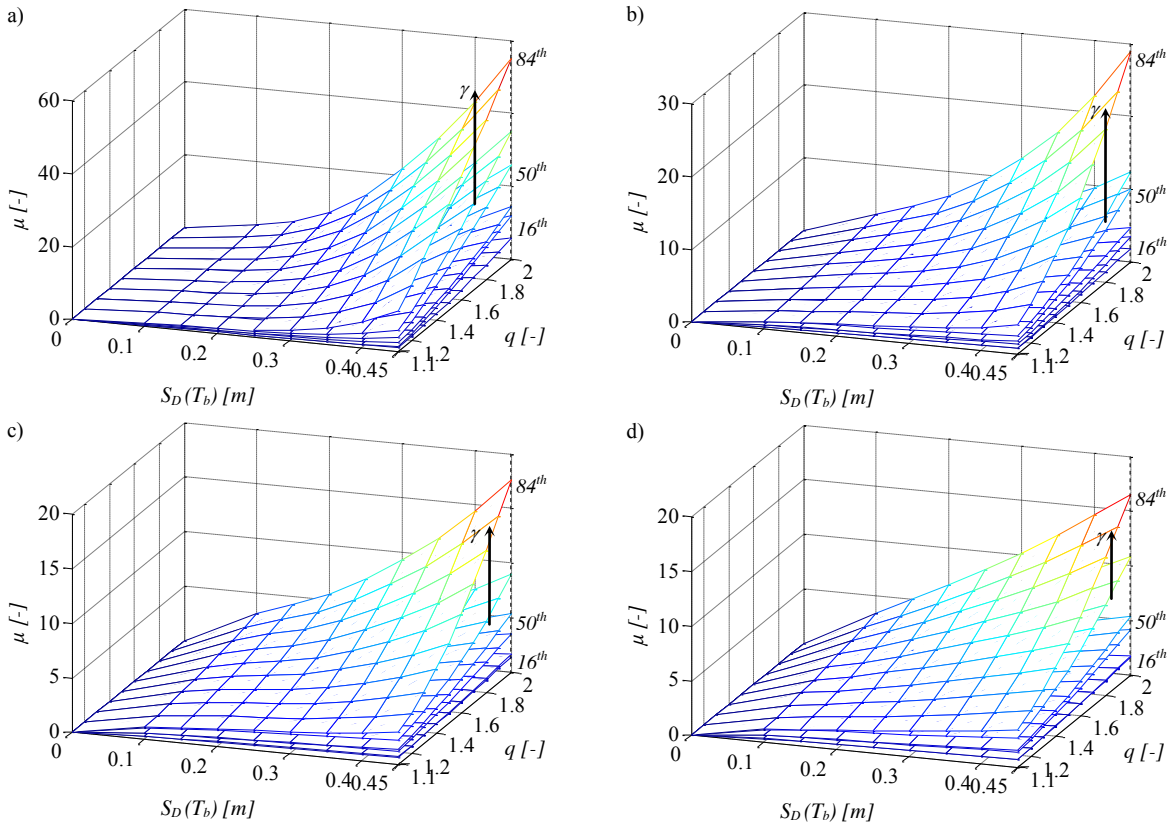

Figure 3: IDA curves of superstructure with I_d=6 and T_b=3 s (a), T_b=4 s (b), T_b=5 s (c), T_b=6 s (d). The arrow denotes the increasing direction of γ = 0.6-0.8.

4.3 Seismic fragility analysis

The following step for the seismic reliability assessment of inelastic buildings isolated by FPS, is the evaluation of the seismic fragility. The seismic fragility can be defined as the probabilities P_f exceeding different limit states at each level of the intensity measure *IM*. For this reason the limit state thresholds need to be defined. In particular, the performance levels of the isolation system are assumed in terms of radius in plan of the concave surface, r [m] (Tab. 2); while, the performance levels of the equivalent system superstructure are defined in terms of available ductility, μ [-] (Tab. 3) considering structural systems in ordinary conditions and neglecting aging effects [62]-[71].

	$LS_{b,1}$	$LS_{b,2}$	$LS_{b,3}$	$LS_{b,4}$	$LS_{b,5}$	$LS_{b,6}$	$LS_{b,7}$	$LS_{b,8}$	$LS_{b,9}$	$LS_{b,10}$
r [m]	0.05	0.1	0.15	0.2	0.25	0.3	0.35	0.4	0.45	0.5
$p_f(50\ years)=1.5\cdot10^{-3}$										

Table 2: Limit state thresholds for the isolation level.

	$LS_{\mu,1}$	$LS_{\mu,2}$	$LS_{\mu,3}$	$LS_{\mu,4}$	$LS_{\mu,5}$	$LS_{\mu,6}$	$LS_{\mu,7}$	$LS_{\mu,8}$	$LS_{\mu,9}$	$LS_{\mu,10}$
μ [-]	1	2	3	4	5	6	7	8	9	10
$p_f(50\ years)=2.2\cdot10^{-2}$										

Table 3: Limit state thresholds for the superstructure.

Fig.s 4-5 show the fragility curves regarding the isolation level and the superstructure. Each figure contains several curves corresponding to the different values of the mass ratio and strength reduction factors q, considered in this study. Only the results corresponding to some limit state thresholds and to T_b=3, 6 s are reported because of space constraints. Generally, the seismic fragility decreases for increasing the limit state thresholds. The curves reflect the same trend of the IDA curves.

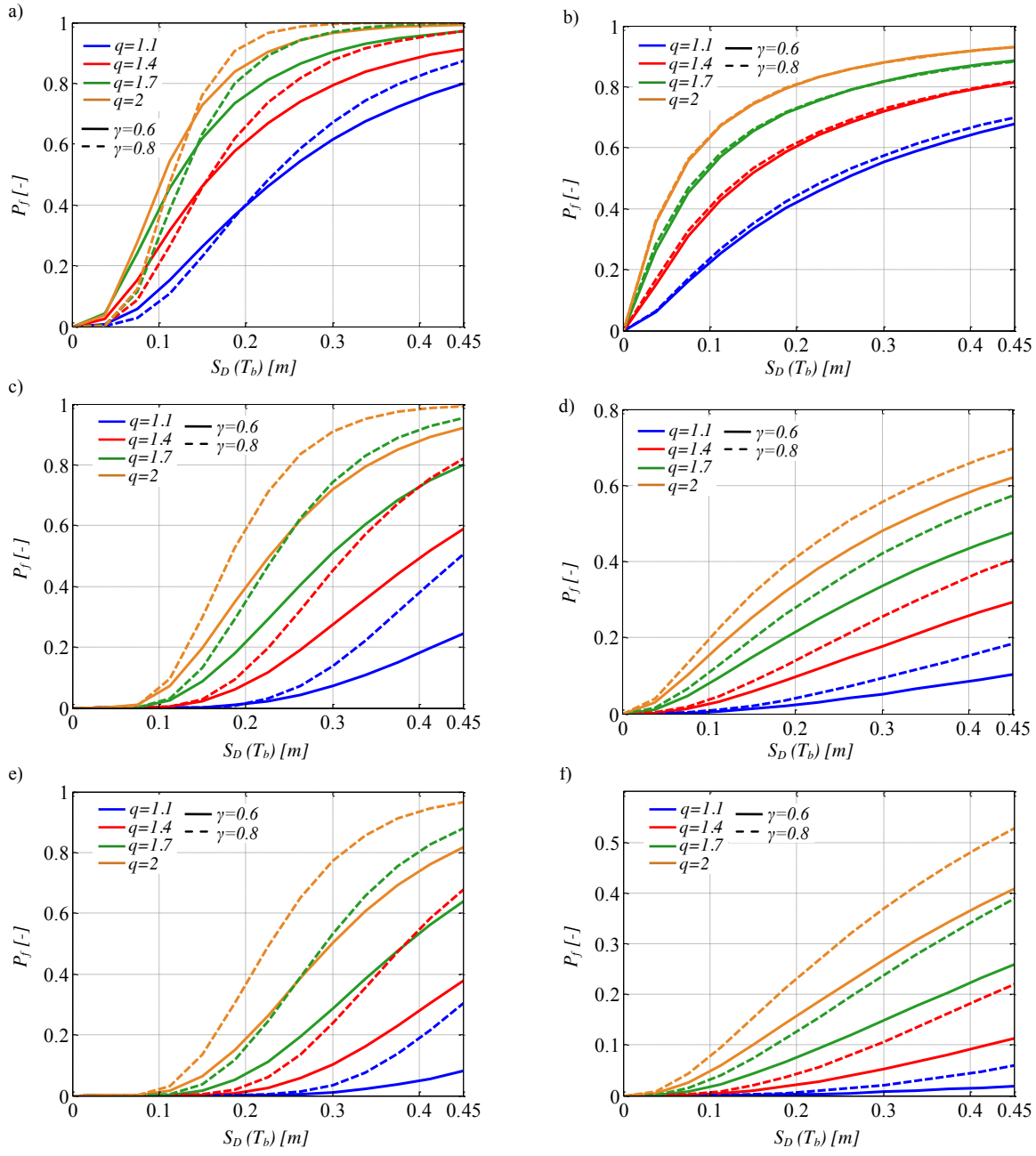

Figure 4: Seismic fragility curves of the superstructure related to I_d=6 for $L_{\mu,1}$=1 and T_b =3 s (a), $L_{\mu,1}$=1 and T_b =6 s (b), $L_{\mu,3}$=3 and T_b =3 s (c), $L_{\mu,3}$=3 and T_b =6 s (d), $L_{\mu,5}$=5 and T_b =3 s (e), $L_{\mu,5}$=5 and T_b =6 s (f).

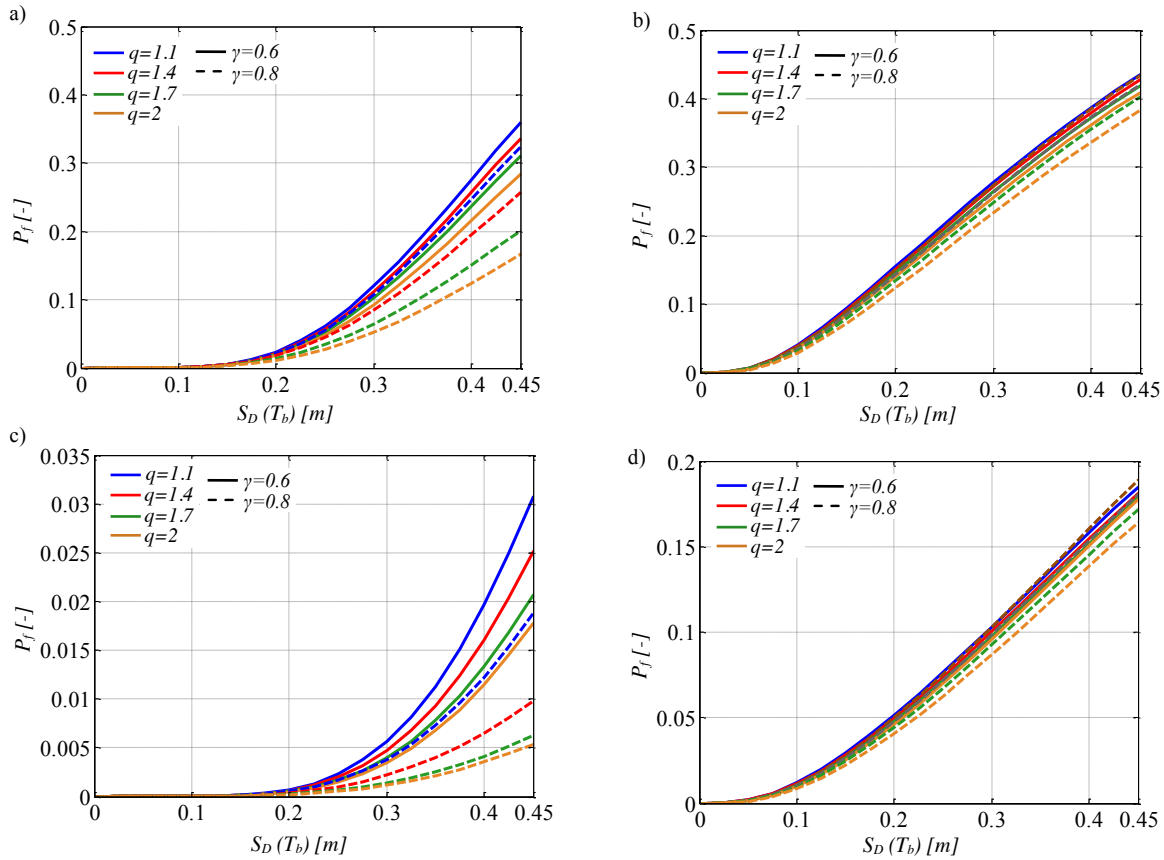

Figure 5: Seismic fragility curves of the isolation level related to I_d=6 for $L_{Sb,4}$=0.2 m and T_b =3 s (a), $L_{Sb,4}$=0.2 m and T_b =6 s (b), $L_{Sb,8}$=0.4 m and T_b =3 s (c), $L_{Sb,8}$=0.4 m and T_b =6 s (d).

4.4 Site seismic hazard

The local seismic hazard of L'Aquila site (Italy), soil class B, with geographic coordinates 42°38'49''N and 13°42'25''E, has been considered. The seismic hazard curves (Fig. 6), expressed in terms of $IM = S_D(T_b)$ and related to the four values of the isolated periods analysed in the parametric study, have been realized according to NTC08 [37]. Each curve represents the average values of the annual rate λ_s of exceeding the *IM* level.

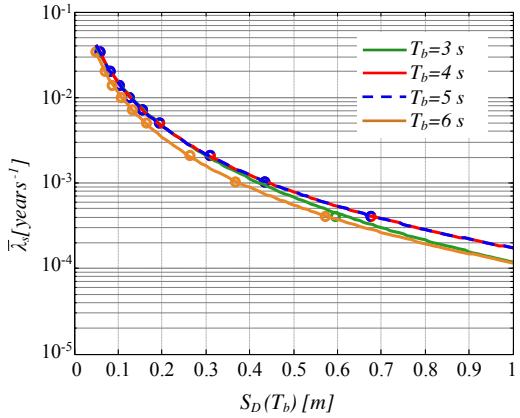

Figure 6: Seismic hazard curves related to the different isolated periods T_b for L'Aquila site (Italy).

4.5 Seismic reliability analysis

Integrating the previously defined fragility curves with the seismic hazard curve, expressed in terms of the same *IM*, related to the reference site, allows to calculate the mean annual rates of exceeding the limit states. These latter ones have to be transformed into probabilities of exceedance in the time frame of interest (e.g., 50 years) by using a Poisson distribution in order to evaluate the seismic reliability of the base-isolated structures equipped with FP devices.

In Fig. 7-8, the linear regressions of the curves representing the seismic reliability (structural performance (SP) curves) of the isolation level and of the superstructure are plotted in logarithmic scale for the different limit state thresholds in terms of radius in plan r and the displacement ductility μ, respectively, and for different values of mass ratio and (ductility-dependent) strength reduction factor.

Fig. 7 shows the seismic reliability curves of the isolation level. It is possible to observe that, in most of cases, the increase of the (ductility-dependent) strength reduction factor and of the mass ratio leads to a slight increase of the seismic reliability, while an increase of T_b lead to a decrease of the seismic reliability. From these seismic reliability-based design (SRBD) abacuses, it is possible to design the plan dimension of the isolator (i.e., radius in plan r of the concave surface) in order to respect the expected reliability level. In particular, an exceeding probability of $P_f = 1.5 \cdot 10^{-3}$ (related to the collapse limit state, reliability index $\beta = 3$ in 50 years) [46]-[49] is achieved through a radius in plan r ranging from about 0.35 m to about 0.8 m depending on the values of the structural properties.

Fig. 8 represent the seismic reliability (structural performance (SP)) curves of the inelastic superstructure. From these abacuses, it is possible to evaluate the displacement ductility demand as function of q for each parameter combination corresponding to the exceeding probability in 50 years, equal to $2.2 \cdot 10^{-2}$ [46].

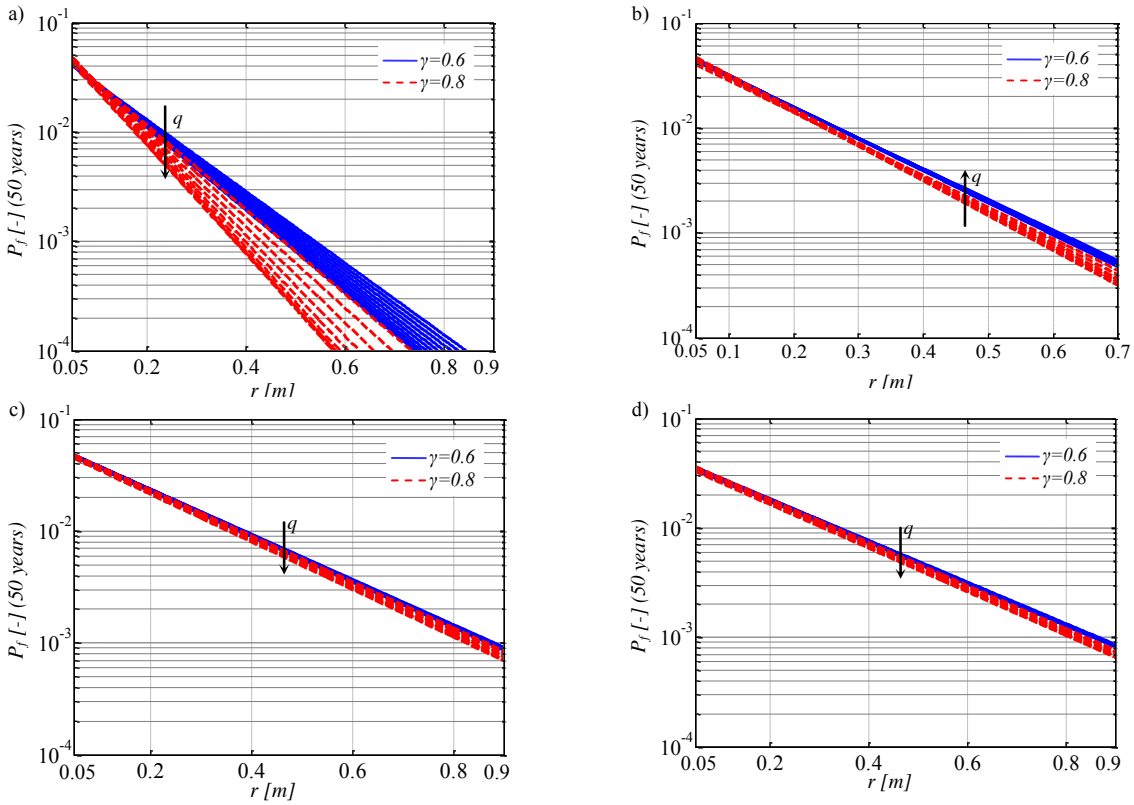

Figure 7: Seismic reliability curves of the isolation level related to I_d=6, for T_b =3 s (a), T_b =4 s (b), T_b =5 s (c), T_b =6 s (d).

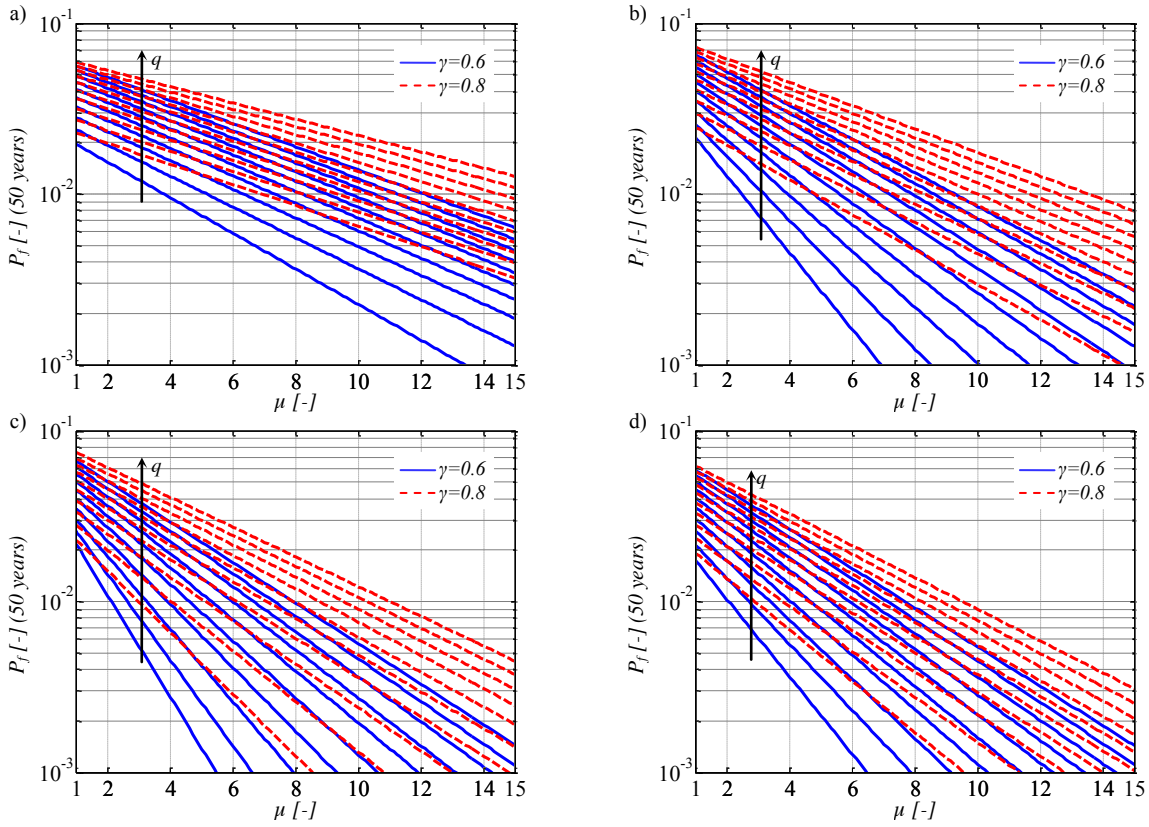

Figure 8: Seismic reliability curves of the isolation level related to I_d=6, for T_b =3 s (a), T_b =4 s (b), T_b =5 s (c), T_b =6 s (d).

In fact, this value of failure probability is related to the life safety limit state , adopted as reference limit state in order to define the seismic intensity of the reference site (L'Aquila, Italy) and design the inelastic characteristics of the several base-isolated structural systems analyzed, as provided by [37] and previously described. The results show that the seismic reliability of the superstructure decreases for higher values of γ, q and T_b. Therefore, it is possible to declare that for some parameter combinations the values of the (ductility-dependent) strength reduction factor q can lead to very high values of the ductility demand for base-isolated systems with FPS also due to the uncertainty on the sliding friction coefficient. Indeed, especially for high mass ratio with low isolated periods, the upper limit value of q should be lower than 1.5. In the hypothesis of regular building frames, these proposed reliability-based design (SRBD) abacuses can be used for the preliminary design of the dimensions in plan of the friction pendulum devices and for the evaluation of the ductility demand of the superstructure depending on structural properties in an area with a seismic hazard similar to that considered. Within the force-based approach for designing new base-isolated systems, the codes [35]-[39] provide behaviour factors which consider both the ductility-dependent and overstrength factors depending on the properties of the superstructure. The results of the seismic reliability analysis in this study, related to both superstructure and isolation devices, represent the corresponding behaviour of the equivalent perfectly elastoplastic models and, therefore, are influenced only by the ductility-dependent term of the behaviour factor recommended by [35]-[39]. Therefore, considering a reduced value of the behaviour factor provided by the provisions [35]-[39], obtained from the ratio with respect to the corresponding overstrength factor recommended by [35]-[39], it is possible to design the FPS properties in compliance with the codes.

5 CONCLUSIONS

This paper deals with the seismic reliability of inelastic structural systems equipped with FPS. The isolated structures are described by employing an equivalent 2dof model characterized by a perfectly elastoplastic rule to account for the inelastic response of the yielding superstructure, whereas, the FPS behavior is described by a velocity-dependent model. Then, incremental dynamic analyses are developed to evaluate the response statistics related to both superstructure and isolation level for different mass ratios and (ductility-dependent) strength reduction factors. The estimates of the response statistics, then, are used for deriving seismic fragility curves for the yielding superstructure and the isolation level assuming different values of the corresponding limit state thresholds. In the final part of the work, considering the seismic hazard curves related to L'Aquila site (Italy), as provided by NTC08, regarding systems with a design life of 50 years, seismic reliability-based (SRBD) abacuses are proposed with the aim to define the radius in plan of the FP isolators and the ductility demand in function of the structural properties and the reliability level expected. From the results of reliability analysis of the superstructure, it is possible to declare that the values of the strength reduction factor for base-isolated systems with FPS should be lower than 1.5.

REFERENCES

[1] C. Christopoulos, A. Filiatrault, *Principles of Passive Supplemental Damping and Seismic Isolation*. IUSS Press: Pavia, Italy, 2006.

[2] Zayas VA, Low SS, Mahin SA. A simple pendulum technique for achieving seismic isolation. *Earthquake Spectra*; **6**:317–33, 1990.

[3] Su L, Ahmadi G, Tadjbakhsh IG. Comparative study of base isolation systems. *Journal of Engineering Mechanic*; **115**:1976–92, 1989.

[4] Mokha A, Constantinou MC, Reinhorn AM. Teflon Bearings in Base Isolation. I: Testing. *J. Struct. Eng.*; **116**(2): 438-454, 1990.

[5] Constantinou MC, Mokha A, Reinhorn AM. Teflon Bearings in Base Isolation. II: Modeling. *J. Struct. Eng.*; **116**(2):455-474, 1990.

[6] Constantinou MC, Whittaker AS, Kalpakidis Y, Fenz DM, Warn GP. Performance of Seismic Isolation Hardware Under Service and Seismic Loading. Tech. Report, 2007.

[7] De Iuliis M., Castaldo P., Palazzo B., Analisi della domanda sismica inelastica del terremoto de L'Aquila su sistemi dimensionati secondo le NTC2008. *Ingegneria Sismica*, Patron Editore **XXVII**(3), 55–68, 2010.

[8] Palazzo B., Castaldo P., Marino I., The Dissipative Column: A New Hysteretic Damper," *Buildings* **5**(1), 163-178, 2015, doi:10.3390/buildings5010163.

[9] Castaldo, P., Palazzo, B., Perri F. FEM simulations of a new hysteretic damper: the dissipative column, *Ingegneria Sismica - International Journal of Earthquake Engineering*, Anno XXXIII – Speciale CTA- 2015- Num. 1-2:34-45.

[10] Castaldo P., *Integrated Seismic Design of Structure and Control Systems*. Springer International Publishing: New York, 2014 . DOI 10.1007/978-3-319-02615-2.

[11] Giugliano M.T., Longo A., Montuori R., Piluso V., Plastic design of CB-frames with reduced section solution for bracing members. *Journal of Constructional Steel Research*. Vol. 66 pp 611-621. 2010.

[12] Montuori R., Nastri E., Piluso V. Theory of plastic mechanism control for the seismic design of braced frames equipped with friction dampers - *Mechanics Research Communications* – Vol. 58. pp. 112-123 2014.

[13] Montuori R., Piluso V., Troisi M. Innovative structural details in MR-frames for free from damage structures *Mechanics Research Communications* –58, 146-156, 2014.

[14] Longo A., Montuori R., Piluso V., Theory of Plastic Mechanism Control of Dissipative Truss Moment Frames, *Engineering Structures*, Vol. 37, pp. 63-75, 2012.

[15] A. Longo, R. Montuori, V. Piluso, Failure mode control and seismic response of dissipative truss moment frames, *Journal of Structural Eng*., **138**(11), 1388-1397, 2012.

[16] Asteris, P.G., Tsaris, A.K., Cavaleri, L., Repapis, C., Papalou, A., Di Trapani, F., Karypidis, D.F. (2015). Prediction of the Fundamental Period of Infilled RC Frame Structures Using Artificial Neural Networks, Computational Intelligence and Neuroscience, Article ID 474106, http://dx.doi.org/10.1155/2016/5104907.

[17] Asteris PG, Cavaleri L, Di Trapani F, Sarhosis V. A macro-modelling approach for the analysis of infilled frame structures considering the effects of openings and vertical loads. Structure and Infrastructure Engineering 2016 12(5): 551-566.

[18] Almazàn JL, De la Llera JC. Physical model for dynamic analysis of structures with FPS isolators. *Earthquake Engineering and Structural Dynamics*; **32**:1157–1184, 2003.

[19] Ayyub BM, McCuen RH. Probability, statistics, and reliability for engineers. 2nd ed. NY: CRC Press; 2002.

[20] Lin YK, Cai GQ. Probabilistic structural dynamics—advanced theory and applications. NY: McGraw-Hill; 1995.

[21] Cavaleri, L., Di Trapani, F., Ferrotto, M.F. A new hybrid procedure for the definition of seismic vulnerability in Mediterranean cross-border urban areas, Natural Hazards, 1-25, 2016.

[22] Asteris, P.G., Cavaleri, L., di Trapani, F., Macaluso, G., Scaduto, G. Definition of seismic vulnerability maps for civil protection systems: The case of lampedusa Island., Open Construction and Building Technology Journal 10 (Suppl 1: M5), 87-105, 2016.

[23] Chen J, Liu W, Peng Y, Li J. Stochastic seismic response and reliability analysis of base-isolated structures. *J Earthquake Eng*; **11**:903 – 24, 2007.

[24] Alhan C, Gavin HP. Reliability of base isolation for the protection of critical equipment from earthquake hazards. *Eng Struct*; **27**:1435 – 49, 2005.

[25] Zou XK, Wang Q, Li G, Chan CM. Integrated reliability-based seismic drift design optimization of base-isolated concrete buildings. *J Struct Eng*; **136**:1282 – 95, 2010.

[26] Mishra SK, Roy BK, Chakraborty S. Reliability-based-design-optimization of base isolated buildings considering stochastic system parameters subjected to random earthquakes. *Int J Mech Sci*; **75**:123 – 33, 2013.

[27] M.T. Giugliano, A. Longo, R. Montuori, V.Piluso, Influence of homoschedasticity hypothesis of structural response parameters on seismic reliability of CB-frames, *Georisk*, **5**(2), 120-131, 2011.

[28] M.T. Giugliano, A. Longo, R. Montuori, V. Piluso, Seismic reliability of traditional and innovative concentrically braced frames, *Earthquake Engineering and Structural Dynamics*, **40**(13), 1455–1474, 2011.

[29] A. Longo, R. Montuori, V. Piluso, Seismic reliability of V-braced frames: Influence of design methodologies, *Earthquake Engineering and Structural Dynamics*, **38**(14), 1587–1608, 2009.

[30] Zhao C, Chen J. Numerical simulation and investigation of the base isolated NPPC building under three-directional seisemic loading. *Nucl Eng Des*; **265**:484 – 96, 2013.

[31] Castaldo P, Palazzo B, Della Vecchia P. Seismic reliability of base-isolated structures with friction pendulum bearings. *Engineering Structures*; **95**:80-93, 2015.

[32] Castaldo P., Palazzo B., Della Vecchia P. Life-cycle cost and seismic reliability analysis of 3D systems equipped with FPS for different isolation degrees, *Engineering Structures*; 125:349–363, 2016. DOI:10.1016/j.engstruct.2016.06.056.

[33] Castaldo P., Amendola G., Palazzo B., Seismic fragility and reliability of structures isolated by friction pendulum devices: seismic reliability-based design (SRBD), *Earthquake Engineering and Structural Dynamics*, **46**(3); 425–446, 2017, DOI: 10.1002/eqe.2798.

[34] Castaldo, P., Palazzo, B., Ferrentino, T., Petrone, G.. Influence of the strength reduction factor on the seismic reliability of structures with FPS considering intermediate PGA/PGV ratios. Composites Part B: Engineering, 2016, http://dx.doi.org/10.1016/j.compositesb.2016.09.072.

[35] Structural Engineering Institute. Minimum design loads for buildings and other structures (Vol. 7, No. 5). Amer Society of Civil Engineers, 2010.

[36] European Committee for Standardization. Eurocode 8-Design of Structures for Earthquake Resistance. Part 1: General Rules, Seismic Actions and Rules for Buildings, Brussels, 2004.

[37] NTC08. Norme tecniche per le costruzioni. Gazzetta Ufficiale del 04.02.08, DM 14.01.08, Ministero delle Infrastrutture.

[38] Japanese Ministry of Land, Infrastructure and Transport, Notification No. 2009–2000, Technical Standard for Structural Specifications and Calculation of Seismically Isolated Buildings 2000.

[39] Quantification of Building Seismic Performance Factors, FEMA P695 / June 2009.

[40] Naeim F, Kelly JM. Design of Seismic Isolated Structures: From Theory to Practice. John Wiley & Sons, Inc.; 1999.

[41] Palazzo B. Seismic Behavior of base-isolated Buildings. Proc. International Meeting on earthquake Protection of Buildings, Ancona, 1991.

[42] Fanaiea N. and Afsar Dizaj E. Response modification factor of the frames braced with reduced yielding segment BRB *Structural Engin. and Mechanics*; **50**(1):1-17, 2014.

[43] Abdollahzadeh, Gh., Banihashemi, M.R. Response modification factor of dual moment-resistant frame with buckling restrained brace (BRB), *Steel Com. Str.*,**14**(6),621-636, 2013.

[44] Niroomandi A., Maheri A. Upgrading the ductility and seismic behavior factor of ordinary rc frames using fiber composite sheets, *Conference: 3rd International Conference on Concrete & Development*, 2009, Tehran, Iran, 587-598.

[45] Collins KR, Stojadinovic B. Limit states for performance-based design. 12WCEE, 2000.

[46] Bertero RD, Bertero VV. Performance-based seismic engineering: the need for a reliable conceptual comprehensive approach. *Earthquake Engineering and Structural Dynamics*; **31**:627–652, 2002 (DOI: 10.1002/eqe.146).

[47] Aoki Y, Ohashi Y, Fujitani H, Saito T, Kanda J, Emoto T, Kohno M. Target seismic performance levels in structural design for buildings. 12WCEE, 2000.

[48] SEAOC Vision 2000 Committee. Performance-based seismic engineering. Report prepared by Structural Engineers Association of California, Sacramento, CA., 1995.

[49] CEN – European Committee for Standardization. Eurocode 0: Basis of Structural Design. Final draft. Brussels, 2006.

[50] Saito T, Kanda J, Kani N. Seismic reliability estimate of building structures designed according to the current Japanese design code. Proc.s of the Str. Eng.s World Congress, 1998.

[51] Cornell CA, Krawinkler H. Progress and challenges in seismic performance assessment. PEER Center News 2000;4(1):1-3

[52] Aslani H, Miranda E. Probability-based seismic response analysis. *Engineering Structures*; **27**(8): 1151-1163, 2005.

[53] Porter KA. An overview of PEER's performance-based earthquake engineering methodology. Proceedings, *Proceedings of the 9th Internat. Conf. on Application of Statistics and Probability in Civil Engin.* (*ICASP9*), San Francisco, California, 2003; 973-980.

[54] Ryan KL, Chopra AK. Estimation of Seismic Demands on Isolators Based on Nonlinear Analysis. J. Struct. Eng., 130(3), 392–402, 2004.

[55] PEER, *Pacific Earthquake Engineering Research Center* http://peer.berkeley.edu/

[56] ITACA, *Italian Accelerometric Archive* http://itaca.mi.ingv.it/ItacaNet/itaca10_links.htm

[57] ISESD, *Internet-Site for European Strong-Motion Data* http://www.isesd.hi.is/ESD_Local/frameset.htm

[58] Mckey MD, Conover WJ, Beckman RJ. A comparison of three methods for selecting values of input variables in the analysis from a computer code. Tec..s; **21**:239-45, 1979.

[59] Vořechovský M, Novák D. Correlation control in small-sample Monte Carlo type simulations I: a simulated annealing approach. *Probabilistic Engineering Mechanics*; **24**(3):452 – 62, 2009.

[60] Celarec D, Dolšek M. The impact of modelling uncertainties on the seismic performance assessment of reinforced concrete frame buildings. *Eng. Str.*; **52**:340 – 354, 2013.

[61] Vamvatsikos D, Cornell CA. Incremental dynamic analysis. *Earthquake Engineering and Structural Dynamics*; **31**(3): 491–514, 2002.

[62] Castaldo, P., Palazzo, B., Mariniello, A.. Effects of the axial force eccentricity on the time-variant structural reliability of aging r.c. cross-sections subjected to chloride-induced corrosion Engineering Structures, **130**: 261-274, 2017.

[63] Etse, G.J., Ripani, M., Vrech, S.M. "Fracture energy-based thermodynamically consistent gradient model for concrete under high temperature," Proceedings of the 8th International Conference on Fracture Mechanics of Concrete and Concrete Structures, FraMCoS 2013, 1506-1515.

[64] Etse, G., Ripani, M., Caggiano, A. & Schicchi, D.S. "Strength and durability of concrete subjected to high temperature: continuous and discrete constitutive approaches," American Concrete Institute, ACI Special Publication 2015-January (SP 305), 9.1-9.18.

[65] Etse, G., Ripani, M. & Mroginski, J.L. "Computational failure analysis of concrete under high temperature," Computational Modelling of Concrete Structures - Proceedings of EURO-C 2014, 2:715-722.

[66] Etse, G., Vrech, S.M. & Ripani, M. "Constitutive theory for Recycled Aggregate Concretes subjected to high temperature," Construction and Building Materials; **111**: 43-53, 2016.

[67] Mroginski, J.L., Etse, G., Ripani, M. "A non-isothermal consolidation model for gradient-based poroplasticity," PANACM 2015 - 1st Pan-American Congress on Computational Mechanics, in conjunction with the 11th Argentine Congress on Computational Mechanics, MECOM 2015, pp. 75-88.

[68] Ripani, M., Etse, G., Vrech, S. & Mroginski, J.L. "Thermodynamic gradient-based poroplastic theory for concrete under high temperature," International Journal of Plasticity; **61**: 157-177, 2014.

[69] Ripani, M., Etse, G., Vrech, S. "Recycled aggregate concrete: localized failure assessment in thermodynamically consistent non-local plasticity framework", Computers and Structures, **178**: 47–57, 2017, doi: 10.1016/j.compstruc.2016.08.007.

[70] Vrech, S.M., Ripani, M. & Etse, G. "Localized versus diffused failure modes in concrete subjected to high temperature," PANACM 2015 - 1st Pan-American Congress on Computational Mechanics, in conjunction with the 11th Argentine Congress on Computational Mechanics, MECOM 2015, pp. 225-236.

[71] Campione, G., Cavaleri, L., Di Trapani, F., Macaluso, G., Scaduto, G. Biaxial deformation and ductility domains for engineered rectangular RC cross-sections: A parametric study highlighting the positive roles of axial load, geometry and materials, Engineering Structures **107**, 116-134, 2016.